Influence of hydrogen on electrical and optical properties of ZnO films

Y. H. Kim[a] S. Zh. Karazhanov[b], and W. M. Kim[a]

[a]*Electronic Materials Center, Korea Institute of Science and Technology, 39-1, Hawolgok-dong, Sungbuk-gu, Seoul 136-791, Korea*

[b]*Institute for Energy Technology, P.O.Box 40, NO-2027 Kjeller, Norway*

Electrical and optical properties of H doped ZnO films have been studied experimentally for different H concentrations before and after annealing, as well as theoretically by first-principles calculations. It is found that electrical resistivity of the H doped ZnO increases when increasing the substrate temperature in the range 25-300 ^{o}C. Carrier concentration and mobility measured by Hall method in as-grown samples are larger than those of annealed ones. The short-wavelength edge of the transmission spectrum of annealed ZnO is found to shift toward lower energies compared to as-grown samples. The band gap estimated from the measured transmission spectra of as grown ZnO increases with increasing H concentration, thus demonstrating the Burstein-Moss effect. However, it decreases in samples annealed at 300 ^{o}C showing suppression of the Burstein-Moss effect. Possible defect models explaining the reason for the suppression are discussed. The results can be explained by formation of H_2 molecules in annealed ZnO.

1. Introduction

Because of its unique optical and electrical properties, such as the low electrical resistivity ($\rho \leq 10^{-3}$ $\Omega \times$cm) and high transparency ($T > 90\%$) in the near ultraviolet (UV) and visible ranges, low material cost, non-toxicity as well as the capability to host large concentrations of hydrogen, semiconducting ZnO has found extensive application as transparent electrodes for photovoltaic solar cells, flat panel displays, low emissivity windows, light emitting diodes, etc.[1-4] H is the ubiquitous impurity in ZnO, which plays important role in the above applications. It is abundantly and unintentionally incorporated during the growth process. H containing ZnO is useful for passivating interface and bulk defects in device structures. For example, commercial Si solar cells fabricated on low cost substrates contain large amounts of defects, which can be detrimental for operation of the cell. H in ZnO can be important for passivating the defects, if ZnO is used as transparent electrodes for the cells. Furthermore, H in ZnO can enhance electrical conductivity. By first-principles calculations it is reported [5-8] that H in ZnO located at the interstitial site or O sites can be a shallow donor, which contributes to electrical conductivity, and it has been confirmed experimentally [9, 10]. The interstitial donor H (H_i) is found to form an O-H complex, which is responsible for the infrared (IR) line 3611 cm^{-1} [11, 12]. Due to small migration energy, the thermal stability of H_i is low [13], which is favourable for the above features.

From the study of kinetics of the IR absorbance corresponding to the O-H complex and of the free carrier concentration, it is found [14, 15] that these parameters decrease with time according to the bimolecular model. This result indicates that the O-H complex is unstable; it can be decomposed and form another more stable complex, which

is IR inactive and does not contribute to free carrier concentration. This complex has been found experimentally in as-grown ZnO and is called "hidden" H [16]. Upon annealing the ZnO near 400 ^{o}C, the "hidden" H has been transformed into O-H complex with the IR line at 3611 cm^{-1}. The O-H complex disappears after annealing at 550 ^{o}C for 30 min and a new line shows up at frequency close to H molecules, i.e. H_2 [11, 17]. According to first-principles calculations, H is suggested to exist in diatomic complex H_2^* (Ref. [18]) form as well, which is less stable than H$_2$. Similar to the "hidden" H, both the molecular H and diatomic H_2^* complex do not enhance the electrical conductivity and cause discrepancy between the concentration of H determined by SIMS and that of free electrons measured by the Hall method.

It should be noted that upon annealing H-related complexes can be transformed or out-diffusion of H can take place. As a result, electrical and optical properties of ZnO can be strongly modified. For example, in as-grown ZnO the increase of H concentration can cause a shift of transmission spectra toward lower wavelength region, which is equivalent to widening of the optical band gap, the so-called Burstein-Moss (BM) effect. Due to this effect the wavelength region where ZnO is transparent is extended. Here we report that upon annealing of the H doped ZnO this effect can be suppressed.

2. Methods

2.1 Experimental details

H doped ZnO films were deposited on glass substrates (Corning Eagle 2000) by radio frequency (rf, 13.56 MHz) planar magnetron sputtering from a sintered ceramic ZnO target at a substrate temperature of 150 ^{o}C. The H doping was done by introducing

H_2 gas into Ar sputtering gas. The relative gas flow rate of H_2 and Ar was adjusted so that the volumetric gas flow ratio, $[H_2]=100\times H_2/(H_2+Ar)$, in the sputter gas varied in the range from 0 to 8 vol.%. The base pressure in the chamber was kept below 5×10^{-5} Pa, and the sputtering deposition was carried out at a pressure of 0.16 Pa. The distance between the target and the substrate was 60 mm, and the rf power density was fixed at 2.5 W/cm^2. The substrate rotated at a constant speed of 12 rpm during sputtering. Annealing was carried out in a rapid thermal processing chamber in vacuum below 10^{-3} Pa for an hour. Film thickness was measured by a surface profilometer after etching away part of the film with diluted HCl solution. The film thicknesses were in the range 272-366 nm. The electrical resistivity, Hall mobility, and electron concentration were determined from Hall-effect measurement using a Van der Pauw method at room temperature. The crystal orientation was inspected by x-ray diffraction (XRD). The optical transmittances were measured using a UV/visible spectrophotometer in the spectral range 250-1100 nm. The specular transmittance (ST) was measured in normal mode of operation whereas the total and diffuse transmittances were monitored using an integrated sphere (IS) module. Since both of the $T(\lambda)$ spectra measured by IS have not been corrected using reference data, they have been used only for comparative analysis and the difference ΔT of $T(\lambda)$ of annealed films from that of as-deposited ones have been analyzed.

2.2 Computational details

The problem has been studied by using the Vienna *ab initio* simulation package (VASP) [19] within the generalized-gradient approximation (GGA) with the multiorbital mean-field Hubbard potential GGA+U [20, 21]. In the computations the parameters U

and *J* accounting for the orbital dependence of the Coulomb and exchange interactions should be entered explicitly as input. Based on analyses of literature (see, e.g. Refs. [22-24]) the calculated band parameters of ZnO *U*=6 eV and *J*=1 eV have been used in band structure calculations. The exchange and correlation energies per electron have been described by the Perdew-Zunger parametrization [25] with the quantum Monte Carlo procedure of Ceperley-Alder [26]. Non-norm-conserving pseudopotentials have been generated in accordance with the projector-augmented-wave (PAW) method [27, 28]. It allowed construction of orthonormalized all-electron-like wave functions for the Zn-3*d*, -4*s*, O -2*s* and -2*p*, and H-1*s* valence electrons.

The computations have been performed for the bulk ZnO in the wurtzite structure with the following optimized lattice parameters $a = b \approx 3.244$ Å, $c/a \approx 1.550$ Å, and $u \approx 0.389$ in satisfactory agreement with experimentally-determined parameters $a = b \approx 3.250$ Å, $c/a \approx 1.602$ Å, and $u \approx 0.382$ [5]. It is well-known that the band gap calculated by DFT is systematically underestimated. By the rigid shift technique, all the conduction band (CB) states have been shifted toward larger energies up to the experimentally determined location 3.44 eV, corresponding to undoped ZnO. The impurity studies have been carried out in 192 and 300 atom supercells with one H_2 molecule, which correspond to concentration of H_2 ~5.0×10^{20} and 3.2×10^{20} cm^{-3}, respectively. Analysis of literature shows that H concentrations in ZnO can be even larger the above ones considered in the computations. H concentration of 2.5×10^{22} cm^{-3} have been reported in electrochemically doped single crystals of ZnO [29]. Smaller H concentrations of ~10^{22} cm^{-3} has been observed in high dose implanted single crystalline ZnO [30]. By rf magnetron sputtering of ZnO the largest H concentration achieved was

$\sim10^{21}$ cm^{-3} [31]. These experimental findings indicate that the above H concentrations considered in the theoretical studies are not far from reality. The defective lattice was fully relaxed using the conjugate-gradient method for the Γ point. Plane-wave cut-off of 290 eV is employed to ensure convergence which is sufficient to reproduce the ground-state and high-pressure structural properties. Convergence was achieved when the forces acting on the atoms were smaller than 10 meV Å^{-1}.

3. Results

3.1 Electrical properties

Figure 1(a) displays the variation of electrical resistivity ρ as a function of the annealing temperature T_a for the ZnO films with [H$_2$]=2%. Here ρ has been determined from the study of kinetics measured for different T_a within the elapsed time of five hours. The value of ρ, corresponding to the stationary state, has been accepted as the one after annealing. Analysis shows that ρ increases slightly with increasing T_a in the range $25<T_a<300$ ^{o}C and increases steeply at $300<T_a<320$ ^{o}C from 10^{-2} to 1.4 $\Omega\times$cm. Upon cooling the sample ρ increases at a slower rate. Upon completion of heating and cooling cycles, ρ increased $\sim$250 times.

Analysis of the above results leads to a perception that the reason for increase of ρ with T_a can be related to modulation of H related defect spectra. To check the validity of the statement, dependence of ρ on [H$_2$] has been studied [Fig. 1(b)] for as-grown and annealed at T=300 ^{o}C ZnO films. It is seen that in as-grown ZnO ρ decreases with increasing [H$_2$]. However, in annealed ZnO the dependence of ρ([H$_2$]) is non-

monotonic, i.e. it increases at smaller [H$_2$] and decreases at larger [H$_2$]. However, ρ in as-grown ZnO remains much smaller than that of annealed ZnO.

To examine the reason for the modulation of electrical resistivity in Fig. 1(b), carrier concentration n and Hall mobility μ have been measured and the results are shown in Fig. 1(c) and (d). It is seen that, in as-grown ZnO, n and μ monotonically increase with increasing [H$_2$] in agreement with previous experimental findings [32]. However, in annealed ZnO, the dependencies $n[H_2]$ and $\mu[H_2]$ are non-monotonic. $n[H_2]$ and $\mu[H_2]$ decrease with increasing [H$_2$] for [H$_2$] <2%, and increase for [H$_2$]>2%. These analyses demonstrate that the modulations of ρ can be related to those of carrier concentration for which H is responsible.

Analysis of [Figs. 1 (a)-(c)] shows that electrical resistivity and carrier concentrations of as-grown and annealed ZnO differ considerably from each other. The reason for the experimental finding can be related to activation of H diffusion, formation of the H-related complexes and/or out-diffusion of H from ZnO, none of which contribute to free carrier concentration.

3.2 XRD spectra

It should be noted that the major defects governing free electron concentration might be not only the H, but also the oxygen vacancies. To clarify this point XRD measurements have been performed. All the XRD spectra showed only one 2θ peak around 34.4^o (Fig. 2), indicating that crystallites of the ZnO:H films form a typical wurtzite structure with (002) preferred orientation normal to the substrate. For convenience of analysis, the location of the (002) peaks in Fig. 2 has been plotted as a

function of [H$_2$] (Fig. 3). Analysis of Fig. 3 shows that upon adding H$_2$ into the sputter gas, the 2θ position of the (002) peak shifts [33]. When increasing the H$_2$ content in the sputter gas the position of the peak shifts towards lower angles, which is consistent with theoretical calculation [5] and experimentally observed results in ZnO:Al films co-doped with H [31]. This result indicates expansion of the lattice along the *c* axis and can be related to increasing the carrier concentration due to the shallow donor interstitial H. However, after vacuum-annealing at T=300 ^{o}C, the (0002) peak position increases towards higher angles, which means lattice shrinkage. The shift of the peak position increases when increasing the H$_2$ concentration.

3.3 Optical properties

In order to see how the optical properties have been changed, transmission spectra $T(\lambda)$ have been measured for the as-grown and the annealed ZnO films with different [H$_2$] in the range 0-8%. It is found that annealing caused shift of the short wavelength edge of $T(\lambda)$ towards longer wavelengths and the relative amount of shift increases with increasing [H$_2$]. Figure 4 (a) presents specular $T(\lambda)$ for the ZnO film with [H$_2$]=8%, which shows the largest shift. The magnitude of the shift of $T(\lambda)$ can be characterized by modulations of the optical band gap. The shift indicates a reduction of the optical gap. For convenience of analysis the $T(\lambda)$ plot has been enlarged in the inset of Fig. 4 (a), which is plotted only for close vicinity of the sharp increase of $T(\lambda)$. The steeply varying part of $T(\lambda)$ has been fitted by a straight line. From the intersection of the straight line with abscissa band gap was estimated for the as-grown and annealed samples. Detailed analysis and discussion on the band gap related issue will be addressed later on.

Figure 4(b) displays the variation in specular transmission averaged in the 400-1100 nm wavelength range with respect to [H$_2$] concentration. Analysis shows that the averaged $T(\lambda)$ of as-deposited ZnO:H film is larger than that of annealed one. This result indicates the possibility of annealing-induced reduction of the optical transparency of the ZnO:H films, which may be related to transformation of H-related defects.

It is important to clarify that the reduction in transmittance upon annealing is not caused by surface scattering due to increased surface roughness after annealing. For experimental verification of this point, total and diffused $T(\lambda)$ has been measured using an IS module. In Figure 5, diffuse transmittance spectra of the as-grown and the annealed ZnO:H films deposited at [H$_2$]=6% are compared. It can be clearly seen that the diffuse transmittance of as-grown film is fairly small being around 1%, which means that the films considered in this paper are very smooth. For all the films studied in this paper, the diffuse transmittances averaged in 400-1100 nm range do not exceed 1.2%. Also, it is noted that the diffuse transmittance of annealed films is almost similar to or even slightly lower than that of as-grown films (see inset in fig. 5). This clearly shows that the surface roughness remains relatively unchanged even after annealing for all the films, indicating that surface scattering is not the major cause of annealing-induced reduction in transmittance.

Now, the shift of the $T(\lambda)$ spectra towards lower energies shall be analyzed, which, as noted above, can be characterized by modulation of the optical band gap. The band gaps estimated from both the specular and the diffuse $T(\lambda)$ spectra are presented in Figure 6 as a function of [H$_2$] concentration in the range 0-8%. For all the films, the differences in optical band gaps determined by two methods are less than 1%, which

again shows that our films have smooth surface, and that the influence of surface roughness on optical spectra can be neglected. The band gap of as-grown samples increases with increasing [H_2] in agreement with previous findings [32]. The reason might be the well-known BM effect [32], because the carrier concentrations are larger than the Mott critical concentration ~3-4×10^{18} cm^{-3}. However, upon annealing the band gap is decreased [Fig. 6], which means suppression of the BM effect.

3.4 Discussion

Here we discuss a few different models for the H-related effects in ZnO, which may be applicable for explaining the suppression of the BM effect upon vacuum annealing of H doped ZnO. However, the number of the models explaining the result is not limited to this list.

Out-diffusion of H from ZnO. One of the models is out-diffusion of H from ZnO during annealing. This causes a shift of the Fermi level toward lower energies thus leading to reverse BM effect and explains the difference in electrical properties of as-grown and annealed ZnO films [Fig. 1]. The model based on out-diffusion of H is consistent with some experimental findings. One of them is decrease of the O-H signal even at 400 ^{o}C [12]. In rf magnetron sputtered ZnO:Al films co-doped with H, the hydrogen content determined from the analysis of secondary ion mass spectroscopy (SIMS) decreased substantially after both air- and vacuum-annealing at 300 ^{o}C [31].

Oxygen vacancy. V_O is well-known to cause *n*-type electrical conductivity of ZnO.[8, 34, 35]. As noted above, H located at the O site (H_O) can also be a shallow donor [6]. If that was the case in our samples, then V_O would be formed during annealing.

Below we discuss the question of whether V_O can cause suppression of the BM effect. First-principles calculations have been performed for V_O in ZnO. Figure 7 presents the band structure of ZnO with V_O in neutral (V_O^0) and positively charged (V_O^+) states. It is seen that V_O^0 and V_O^+ form an intermediate band in the band gap of ZnO. This result agrees with that of Ref. [8]

It should be noted that at the temperature ranges considered in this work, all V_O is expected to be positively charged. If so, then the four Zn atoms nearest to V_O would shift outwards from the vacancy compared to their location in an ideal lattice [8, 35]. In other words, even after annealing lattice expansion should be observed in XRD measurements. However, our results in Figs. 2 and 3 showed lattice shrinkage, which means that V_O is not the defect controlling carrier concentration.

Diatomic H_2^* complex. Another model is the formation of some H-related defects. One example is H_2^* [Fig. 8(a), Ref. [18]. It was suggested in order to explain the failure to detect the "hidden" hydrogen in ZnO. At that time the common agreement was that the hidden species was interstitial H_2, but no experimental confirmation was available. Since then, however, the existence of interstitial H_2 was experimentally confirmed [11] and there is no experimental evidence for the existence of the complex H_2^*. Furthermore our estimation shows that the H_2^* is less stable than the H_2. So, the H_2 molecule seems the most appropriate model, which is capable of explaining our experimental results.

Formation of H_2 molecules. In as-grown ZnO the H can exist in O-H form with dominating vibrational signal 3611 cm^{-1} [11]. However, upon annealing at 550 °C for 30 min a new line at 4145 cm^{-1} has been observed at the expense of the above O-H signal

[11, 17]. The frequency is close to 4161 cm^{-1} belonging to H$_2$ molecules. We suggest that in this particular case formation of H$_2$ molecules is the most suitable model to explain the experimental findings. The band structure for ZnO containing an isolated H$_2$ molecule has been studied [Fig. 7]. Analysis shows that the molecule does not create an energy level in the band gap of ZnO. So, it can cause a reduction of free carrier concentration [Fig. 1], reverse the effect of BM [Fig. 6], as well as explaining why the electrical properties of the as-grown and the annealed ZnO films differ from each other [Fig. 1].

In our samples upon annealing at ~300 ^{o}C some part of H could be combined into molecular H$_2$. According to Refs. [13, 36] out-diffusion of H from the plasma-exposed bulk ZnO has been started upon annealing at temperatures 500-600 ^{o}C. Consequently, H can be still the source for the *n*-type electrical conductivity of ZnO at annealing temperatures around ~300 ^{o}C. Based on these results we suggest that both out-diffusion of H from ZnO and their incorporation into H$_2$ molecules might be possible. Consequently, modulation of ρ can be related to transformation of the H related defect spectra.

4. Summary

From the study of the electrical properties of H doped ZnO films before and after annealing it is found that electrical resistivity of the H doped ZnO increases upon increasing the substrate temperature in the range 0-300 ^{o}C. Hall measurements showed that the reason was in part related to a reduction of the free carrier concentration. The short wavelength edge of the optical transmission of as-grown ZnO is found to shift toward larger photon energies when increasing the H concentration, thus indicating Burstein-Moss effect. However, upon annealing the short wavelength edge of the

transmission spectra shifted toward lower energies compared to as-grown samples, which means a reduction of the band gap, i.e. suppression of the Burstein-Moss effect. Possible H-related defect models explaining this effect have been discussed. The H_2 molecule is suggested to be the most suitable defect explaining the experimental results.

Acknowledgments

References

1. D. C. Look, G. C. Farlow, P. Reunchan, S. Limpijumnong, S. B. Zhang and K. Nordlund, Phys. Rev. Lett. **95** (22), 225502 (2005).

2. F.-J. H. T. Söderström, X. Niquille, C. Ballif,, Prog. Photovolt: Res. Appl. **17** (3), 165 (2009).

3. D. C. Look, Mater. Sci. Eng., B **80** (1-3), 383 (2001).

4. W. Beyer, J. Hupkes and H. Stiebig, Thin Solid Films **516** (2-4), 147 (2007).

5. C. G. Van de Walle, Phys. Rev. Lett. **85** (5), 1012 (2000).

6. A. Janotti and C. G. Van de Walle, Nature Mater. **6** (1), 44 (2007).

7. H. Takenaka and D. J. Singh, Phys. Rev. B **75** (24), 241102 (2007).

8. F. Oba, A. Togo, I. Tanaka, J. Paier and G. Kresse, Phys. Rev. B **77** (24), 245202 (2008).

9. D. M. Hofmann, A. Hofstaetter, F. Leiter, H. J. Zhou, F. Henecker, B. K. Meyer, S. B. Orlinskii, J. Schmidt and P. G. Baranov, Phys. Rev. Lett. **88** (4), 045504 (2002).

10. F. A. Selim, M. H. Weber, D. Solodovnikov and K. G. Lynn, Phys. Rev. Lett. **99** (8), 085502 (2007).

11. E. V. Lavrov, F. Herklotz and J. Weber, Phys. Rev. Lett. **102** (18), 185502 (2009).

12. E. V. Lavrov, J. Weber, F. Borrnert, C. G. Van de Walle and R. Helbig, Phys. Rev. B **66** (16), 165205 (2002).

13. M. G. Wardle, J. P. Goss and P. R. Briddon, Phys. Rev. Lett. **96** (20), 205504 (2006).

14. S. J. Jokela and M. D. McCluskey, Phys. Rev. B **72** (11), 113201 (2005).

15. M. D. McCluskey, S. J. Jokela, K. K. Zhuravlev, P. J. Simpson and K. G. Lynn, Appl. Phys. Lett. **81** (20), 3807 (2002).

16. G. A. Shi, M. Saboktakin, M. Stavola and S. J. Pearton, Appl. Phys. Lett. **85** (23), 5601 (2004).

17. E. V. Lavrov, F. Herklotz and J. Weber, Phys. Rev. B **79** (16), 165210 (2009).

18. S. Z. Karazhanov and A. G. Ulyashin, Phys. Rev. B **78**, 085213 (2008).

19. J. P. Perdew and A. Zunger, Phys. Rev. B **23** (10), 5048 (1981).

20. S. Z. Karazhanov, P. Ravindran, A. Kjekshus, H. Fjellvag, U. Grossner and B. G. Svensson, J. Appl. Phys. **100** (4), 043709 (2006).

21. S. Z. Karazhanov, P. Ravindran, A. Kjekshus, H. Fjellvag and B. G. Svensson, Phys. Rev. B **75** (15), 155104 (2007).

22. W. R. L. Lambrecht, A. V. Rodina, S. Limpijumnong, B. Segall and B. K. Meyer, Phys. Rev. B **65** (7), 075207 (2002).

23. D. M. Ceperley and B. J. Alder, Phys. Rev. Lett. **45** (7), 566 (1980).

24. P. E. Blöchl, Phys. Rev. B **50**, 17953 (1994).

25. G. Kresse and D. Joubert, Phys. Rev. B **59** (3), 1758 (1999).

26. G. Kresse and J. Hafner, Phys. Rev. B **47** (1), 558 (1993).

27. V. I. Anisimov, I. V. Solovyev, M. A. Korotin, M. T. Czyzyk and G. A. Sawatzky, Phys. Rev. B **48** (23), 16929 (1993).

28. S. L. Dudarev, G. A. Botton, S. Y. Savrasov, C. J. Humphreys and A. P. Sutton, Phys. Rev. B **57** (3), 1505 (1998).

29. J. Cizek, N. Zaludova, M. Vlach, S. Danis, J. Kuriplach, I. Prochazka, G. Brauer, W. Anwand, D. Grambole, W. Skorupa, R. Gemma, R. Kirchheim and A. Pundt, J. Appl. Phys. **103** (5), 053508 (2008).

30. E. V. Monakhov, A. Y. Kuznetsov, J. S. Christensen, K. Maknys and B. G. Svensson, Superlattices Microstruct. **38** (4-6), 472 (2005).

31. S. H. Lee, T. S. Lee, K. S. Lee, B. Cheong, Y. D. Kim and W. M. Kim, J. Phys.: D: Appl. Phys. **41** (9), 095303 (2008).

32. L.-Y. Chen, W.-H. Chen, J.-J. Wang, F. C.-N. Hong and Y.-K. Su, Appl. Phys. Lett. **85** (23), 5628 (2004).

33. K. Ellmer, J. Phys. D: Appl. Phys. **33** (4), R17 (2000).

34. Y. S. Kim and C. H. Park, Phys. Rev. Lett. **102** (8), 086403 (2009).

35. S. Lany and A. Zunger, Phys. Rev. B **72** (3), 35215 (2005).

36. K. Ip, M. E. Overberg, Y. W. Heo, D. P. Norton, S. J. Pearton, C. E. Stutz, B. Luo, F. Ren, D. C. Look and J. M. Zavada, Appl. Phys. Lett. **82** (3), 385 (2003).
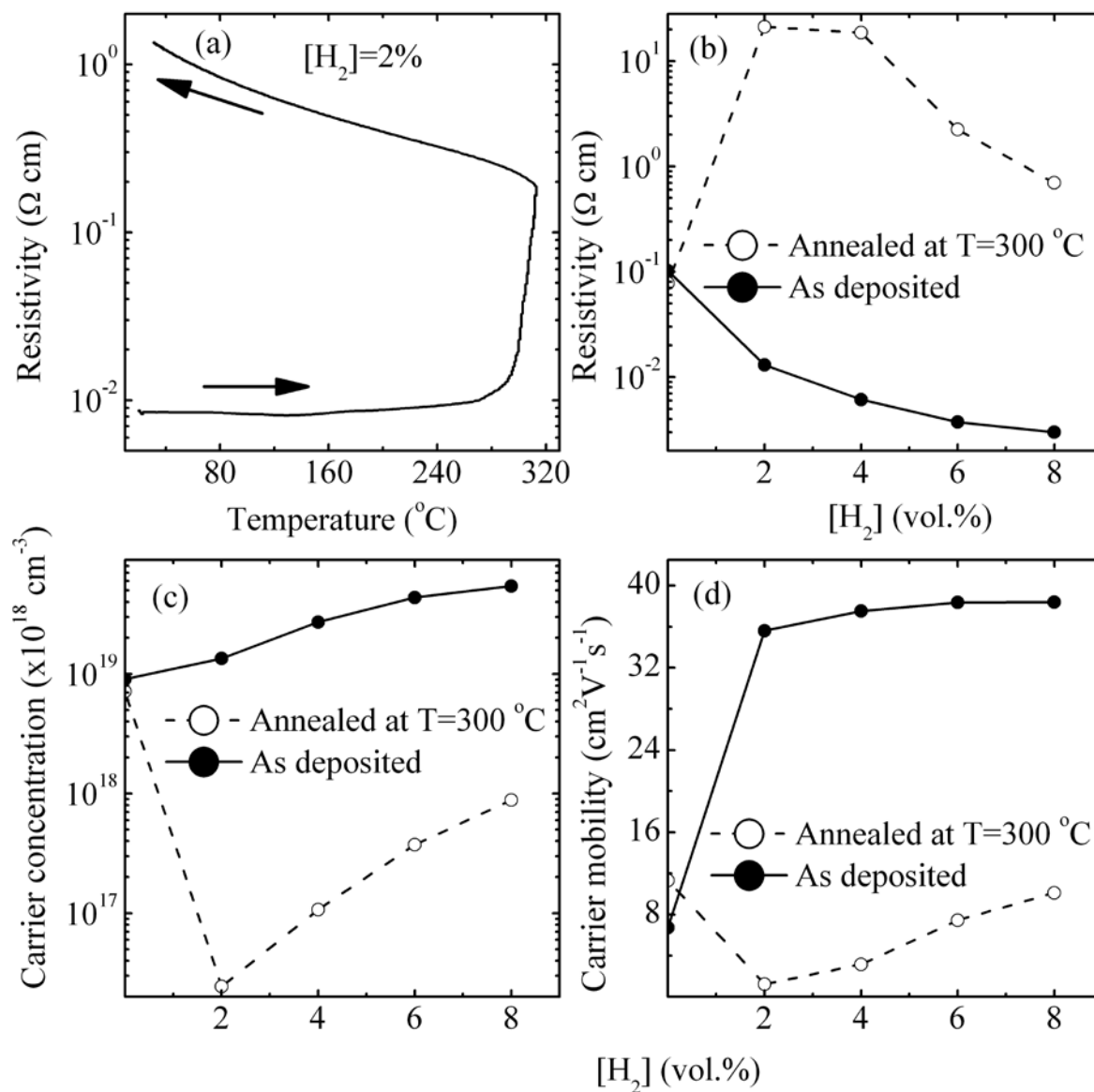
Fig. 1. (a) Dependence of electrical resistance on substrate temperature within 30 min in vacuum for 300 nm thick ZnO films with [H_2]=2% deposited by planar magnetron sputtering at substrate temperature T=150 $^\circ$C. Variation of (b) electrical resistivity, (c) carrier concentration, and (d) carrier mobility as a function of volumetric H_2 flow ratio $H_2/(H_2+Ar)$ for the ZnO films.
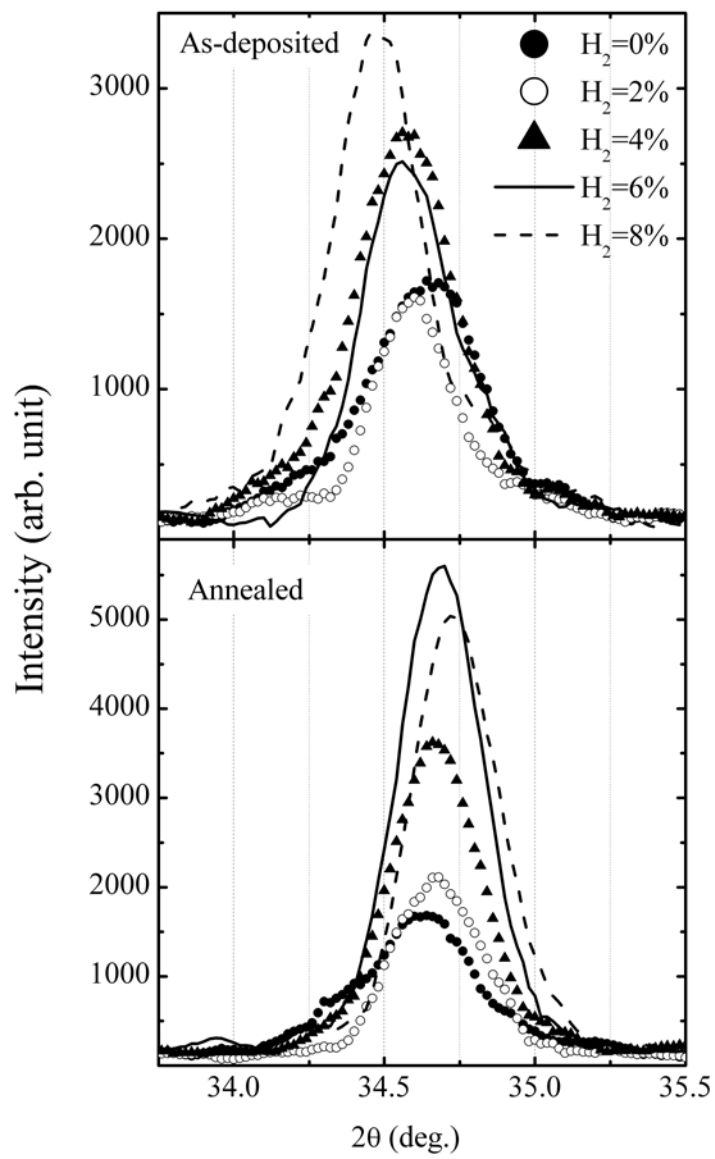
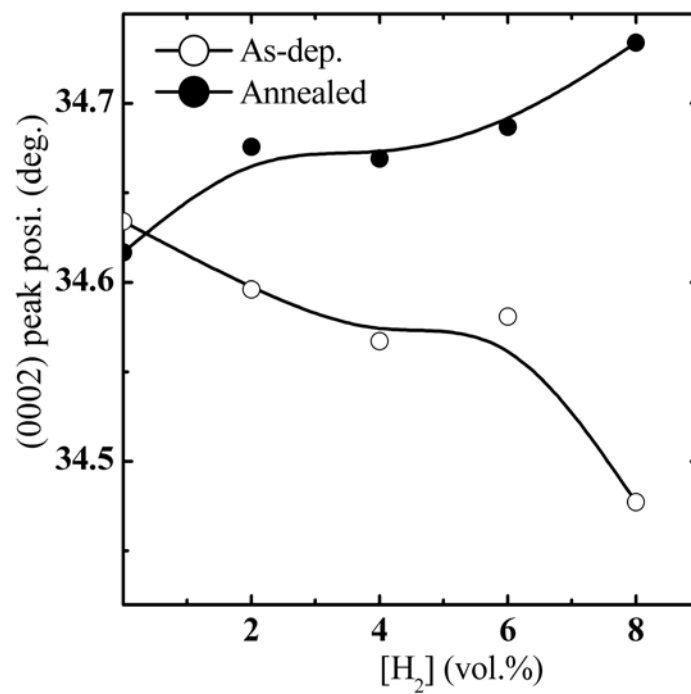Fig. 2. X-ray diffraction patterns of ZnO for different [H_2] concentrations.

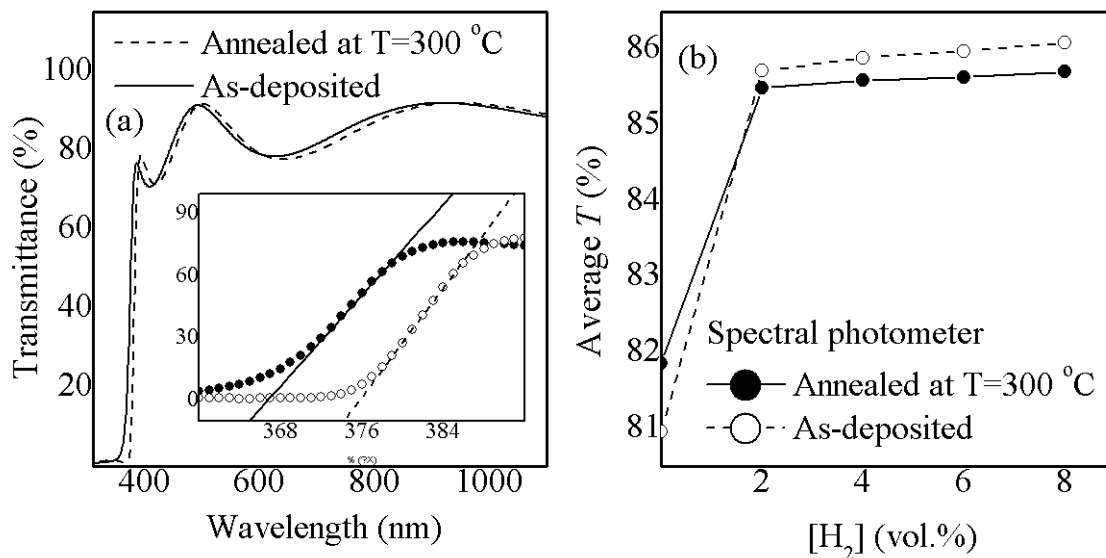Fig. 3. Position of the (0002) peak as a function of the [H_2] concentration.

Fig. 4. (a) Specular transmittance spectra of the as-deposited and annealed at T=300 ^{o}C ZnO films with [H$_2$]= 8%. In the inset the way of estimation of the band gap is demonstrated. Band gap has been estimated from intersection of the straight lines. The experimental data points have been measured on 0.2 nm interval for [H$_2$]=8%. For convenience of analysis each fourth point of the experimental data points have been plotted in the figures in the inset. (b) Specular transmission averaged in the 400-1100 nm wavelength range as a function of [H$_2$].
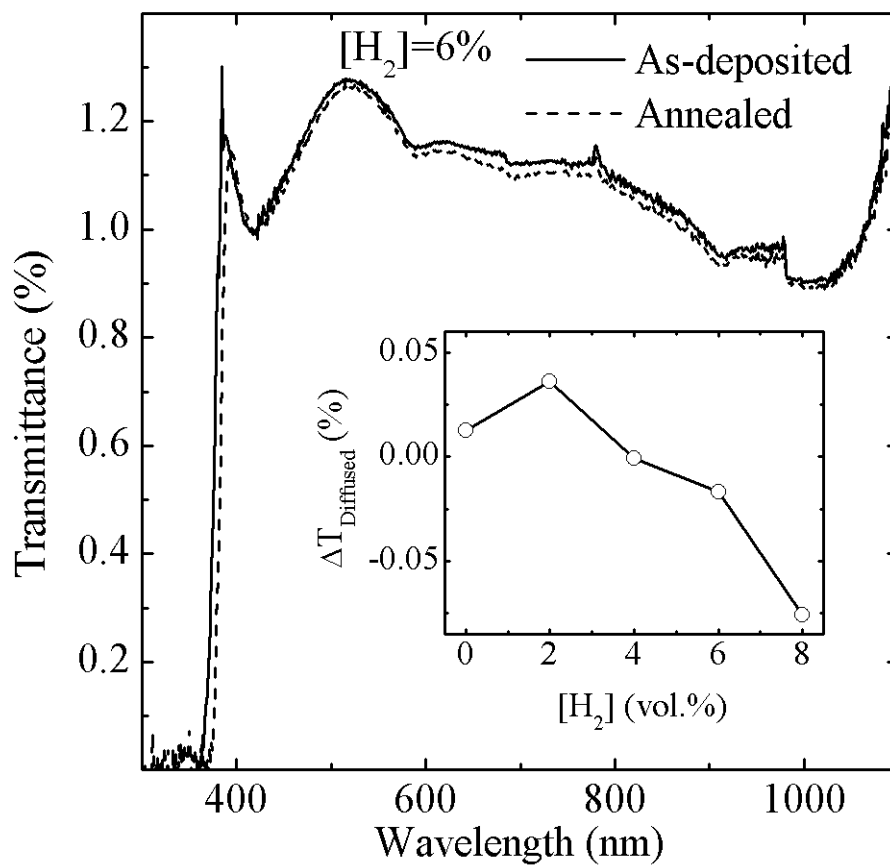
Fig. 5. Total and diffused transmittance spectra $T(\lambda)$ measured by using the IS module. Difference ΔT of the $T(\lambda)$ spectra for annealed ZnO from that of as-deposited one measured using the IS module.
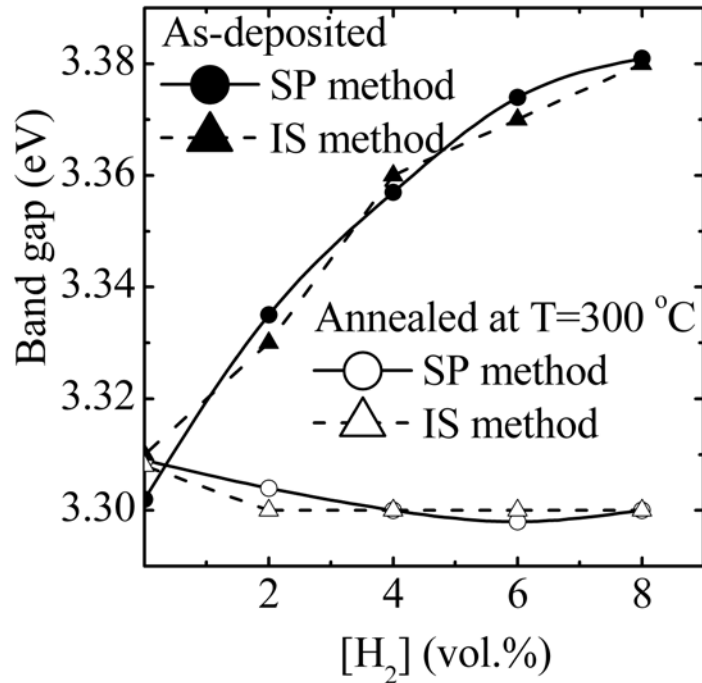
Fig. 6. Optical band gaps of ZnO films with different [H$_2$] concentrations estimated from the dependence $T(\lambda)$ measured by SP and IS methods.
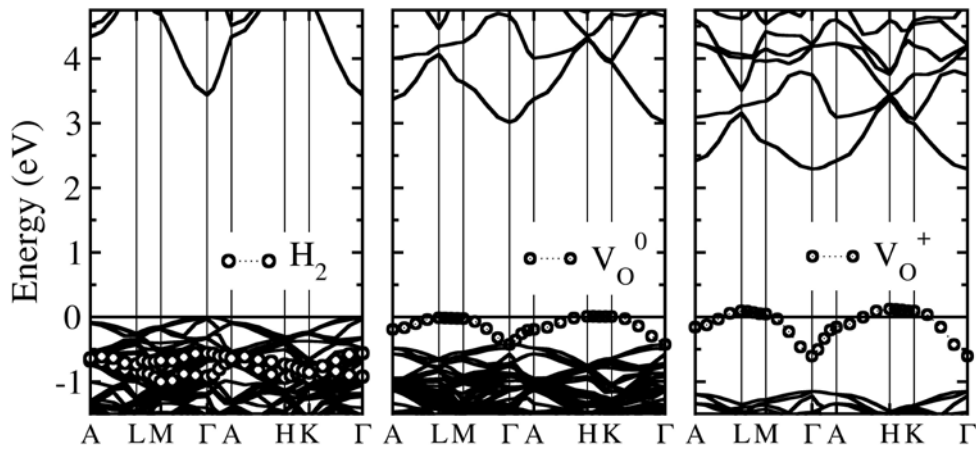
Fig. 7. Band dispersion for ZnO with a H_2 molecule, V_O^0 and V_O^+. The bands plotted by dots ($\circ$)

correspond to H_2, V_O^0, and V_O^+.

References

[1] D. C. Look, G. C. Farlow, P. Reunchan, S. Limpijumnong, S. B. Zhang, K. Nordlund, Phys. Rev. Lett. **95**(22), 225502 (2005).

[2] F.-J. H. T. Söderström, X. Niquille, C. Ballif,, Prog. Photovolt: Res. Appl. **17**(3), 165 (2009).

[3] D. C. Look, Mater. Sci. Eng., B **80**(1-3), 383 (2001).

[4] W. Beyer, J. Hupkes, H. Stiebig, Thin Solid Films **516**(2-4), 147 (2007).

[5] C. G. Van De Walle, Phys. Rev. Lett. **85**(5), 1012 (2000).

[6] A. Janotti, C. G. Van De Walle, Nature Mater. **6**(1), 44 (2007).

[7] H. Takenaka, D. J. Singh, Phys. Rev. B **75**(24), 241102 (2007).

[8] F. Oba, A. Togo, I. Tanaka, J. Paier, G. Kresse, Phys. Rev. B **77**(24), 245202 (2008).

[9] D. M. Hofmann, A. Hofstaetter, F. Leiter, H. J. Zhou, F. Henecker, B. K. Meyer, S. B. Orlinskii, J. Schmidt, P. G. Baranov, Phys. Rev. Lett. **88**(4), 045504 (2002).

[10] F. A. Selim, M. H. Weber, D. Solodovnikov, K. G. Lynn, Phys. Rev. Lett. **99**(8), 085502 (2007).

[11] E. V. Lavrov, F. Herklotz, J. Weber, Phys. Rev. Lett. **102**(18), 185502 (2009).

[12] E. V. Lavrov, J. Weber, F. Borrnert, C. G. Van De Walle, R. Helbig, Phys. Rev. B **66**(16), 165205 (2002).

[13] M. G. Wardle, J. P. Goss, P. R. Briddon, Phys. Rev. Lett. **96**(20), 205504 (2006).

[14] S. J. Jokela, M. D. Mccluskey, Phys. Rev. B **72**(11), 113201 (2005).

[15] M. D. Mccluskey, S. J. Jokela, K. K. Zhuravlev, P. J. Simpson, K. G. Lynn, Appl. Phys. Lett. **81**(20), 3807 (2002).

[16] G. A. Shi, M. Saboktakin, M. Stavola, S. J. Pearton, Appl. Phys. Lett. **85**(23), 5601 (2004).

[17] E. V. Lavrov, F. Herklotz, J. Weber, Phys. Rev. B **79**(16), 165210 (2009).

[18] S. Z. Karazhanov, A. G. Ulyashin, Phys. Rev. B **78**085213 (2008).

[19] G. Kresse, J. Furthmüller, Phys. Rev. B **54**(16), 11169 (1996).

[20] V. I. Anisimov, I. V. Solovyev, M. A. Korotin, M. T. Czyzyk, G. A. Sawatzky, Phys. Rev. B **48**(23), 16929 (1993).

[21] S. L. Dudarev, G. A. Botton, S. Y. Savrasov, C. J. Humphreys, A. P. Sutton, Phys. Rev. B **57**(3), 1505 (1998).

[22] S. Z. Karazhanov, P. Ravindran, A. Kjekshus, H. Fjellvag, U. Grossner, B. G. Svensson, J. Appl. Phys. **100**(4), 043709 (2006).

[23] S. Z. Karazhanov, P. Ravindran, A. Kjekshus, H. Fjellvag, B. G. Svensson, Phys. Rev. B **75**(15), 155104 (2007).

[24] W. R. L. Lambrecht, A. V. Rodina, S. Limpijumnong, B. Segall, B. K. Meyer, Phys. Rev. B **65**(7), 075207 (2002).

[25] J. P. Perdew, A. Zunger, Phys. Rev. B **23**(10), 5048 (1981).

[26] D. M. Ceperley, B. J. Alder, Phys. Rev. Lett. **45**(7), 566 (1980).

[27] P. E. Blochl, Phys. Rev. B **50**(24), 17953 (1994).

[28] G. Kresse, D. Joubert, Phys. Rev. B **59**(3), 1758 (1999).

[29] J. Cizek, N. Zaludova, M. Vlach, S. Danis, J. Kuriplach, I. Prochazka, G. Brauer, W. Anwand, D. Grambole, W. Skorupa, R. Gemma, R. Kirchheim, A. Pundt, J. Appl. Phys. **103**(5), 053508 (2008).

[30] E. V. Monakhov, A. Y. Kuznetsov, J. S. Christensen, K. Maknys, B. G. Svensson, Superlattices Microstruct. **38**(4-6), 472 (2005).

[31] S. H. Lee, T. S. Lee, K. S. Lee, B. Cheong, Y. D. Kim, W. M. Kim, J. Phys.: D: Appl. Phys. **41**(9), 095303 (2008).

[32] L.-Y. Chen, W.-H. Chen, J.-J. Wang, F. C.-N. Hong, Y.-K. Su, Appl. Phys. Lett. **85**(23), 5628 (2004).

[33] K. Ellmer, J. Phys. D-Appl. Phys. **33**(4), R17 (2000).

[34] Y. S. Kim, C. H. Park, Phys. Rev. Lett. **102**(8), 086403 (2009).

[35] S. Lany, A. Zunger, Phys. Rev. B **72**(3), 35215 (2005).

[36] K. Ip, M. E. Overberg, Y. W. Heo, D. P. Norton, S. J. Pearton, C. E. Stutz, B. Luo, F. Ren, D. C. Look, J. M. Zavada, Appl. Phys. Lett. **82**(3), 385 (2003).